

## BSA/HSA ratio modulates the properties of Ca<sup>2+</sup>-induced cold gelation scaffolds



Artur Ribeiro <sup>a,b</sup>, Vadim Volkov <sup>a</sup>, Mariana B. Oliveira <sup>c,d</sup>, Jorge Padrão <sup>a</sup>, João F. Mano <sup>c,d</sup>, Andreia C. Gomes <sup>b</sup>, Artur Cavaco-Paulo <sup>a,\*</sup>

<sup>a</sup> CEB-Centre of Biological Engineering, University of Minho, 4710-057 Braga, Portugal

<sup>b</sup> CBMA (Centre of Molecular and Environmental Biology), Department of Biology, University of Minho, Campus of Gualtar, 4710-057 Braga, Portugal

<sup>c</sup> B's Research Group—Biomaterials, Biodegradables, and Biomimetics, University of Minho, Headquarters of the European Institute of Excellence on Tissue Engineering and Regenerative Medicine, AvePark, 4806-909 Taipas, Guimarães, Portugal

<sup>d</sup> ICVS/3B's—PT Government Associate Laboratory, Braga/Guimarães, Portugal

### ARTICLE INFO

#### Article history:

Received 13 January 2016

Received in revised form 3 May 2016

Accepted 4 May 2016

Available online 6 May 2016

#### Keywords:

Tunable scaffolds

Hydrophobic/Hydrophilic ratio

Induced cold gelation

Surface wettability

Mechanical properties

Cell proliferation

### ABSTRACT

An effective tissue engineering approach requires adjustment according to the target tissue to be engineered. The possibility of obtaining a protein-based formulation for the development of multivalent tunable scaffolds that can be adapted for several types of cells and tissues is explored in this work. The incremental substitution of bovine serum albumin (BSA) by human serum albumin (HSA), changing the scaffolds' hydrophilic/hydrophobic ratio, on a previously optimized scaffold formulation resulted in a set of uniform porous scaffolds with different physical properties and associated cell proliferation profile along time. There was a general trend towards an increase in hydrophilicity, swelling degree and *in vitro* degradation of the scaffolds with increasing replacement of BSA by HSA. The set of BSA/HSA scaffolds presented distinct values for the storage (elastic) modulus and loss factor which were similar to those described for different native tissues such as bone, cartilage, muscle, skin and neural tissue. The preferential adhesion and proliferation of skin fibroblasts on the BSA25%HSA75% and HSA100% scaffolds, as predicted by their viscoelastic properties, demonstrate that the BSA/HSA scaffold formulation is promising for the development of scaffolds that can be tuned according to the tissue to be repaired and restored.

© 2016 Elsevier B.V. All rights reserved.

## 1. Introduction

The development and improvement of clinically effective strategies for the regeneration of healthy and functional tissues is the driving motivation in tissue engineering. One of the milestones is the development of three-dimensional polymer scaffolds that will guide cells to organize into tissues.

Ideally, scaffolds for tissue engineering should meet several design criteria: (1) scaffold surface should allow cell adhesion, promote cell growth and retain differentiated cell functions; (2) the scaffolds should be biocompatible: neither the biomaterial nor its degradation by-products should provoke inflammation or toxicity *in vivo*; (3) the scaffold should be biodegradable to be eliminated eventually; (4) the porosity should provide sufficient space for cell adhesion, extracellular matrix regeneration, and min-

imal diffusion constraints during culture, and the pore structure should allow even spatial cell distribution throughout the scaffold to facilitate homogenous tissue formation; (5) the material should be reproducibly processable into three-dimensional structure, and mechanically strong [1].

There are several methodologies being employed towards the construction of 3D scaffolds, each with specificities, advantages and disadvantages. A new approach is the salt-induced cold gelation [2], which takes advantage of the ability of slow salt addition to a heat-denatured protein solution to screen and disperse charges, leading to a reduction in electrostatic repulsions between protein molecules thus inducing gelation. When using divalent cations such as calcium [3], salt addition may also aid in the formation of salt bridges between negatively charged groups in proteins assisting in the gelling process and ultimately improving scaffold properties. As the gelation process is not immediate after salt addition, it is possible to cast the protein solution into a mold with the appropriate properties for the tissue/organ to be regenerated.

\* Corresponding author.

E-mail address: [artur@deb.uminho.pt](mailto:artur@deb.uminho.pt) (A. Cavaco-Paulo).

Using the combination of  $\text{Ca}^{2+}$ -induced cold gelation and an Experimental Design approach, a macroporous protein-based scaffold suitable for tissue engineering was previously obtained [4]. The scaffold constituted by two distinct model proteins, alpha-casein and bovine serum albumin (BSA), and under optimized working conditions (4.19% of BSA and 0.69% of casein for a pH 7.07) showed adequate degradation rates; good swelling ratio; appropriate pore size, porosity and interconnectivity and good biocompatibility supporting cell adhesion and proliferation [4].

Factors governing scaffold design are complex and though it is argued that there is no ideal scaffold design *per se* and each tissue requires a specific matrix design with defined material properties [5], the conceptual construction of a multivalent tunable scaffold is an appealing idea.

For the BSA4.19%/Casein0.69% scaffold, the value range of each analyzed parameter was similar to those found in the literature for other types of scaffolds designed for specific tissue applications. Thus this scaffold was considered as a good base for the design of moldable and tunable scaffolds for several types of cells/tissues as variations on their composition resulted in changes of the measured parameters.

BSA is an acidic single polypeptide protein extensively used in pharmaceutical industry for a variety of applications. It is used as a stabilizer [6], a blocking agent in various immunoassays [7], in microarray technologies [8], in cell culture medium as growth supplement for viral vaccine manufacturing [9] and in nanoparticles for drug delivery [10]. Despite widely used there are studies showing BSA to be a trigger for allergic reactions [11,12].

In this paper, we evaluated the beneficial effect of substituting of BSA by HSA on the physical properties and cell adhesion of a set of BSA/HSA/Casein scaffolds. With the incremental substitution of BSA by HSA we aimed to reduce possible future allergenic reactions of the scaffolds given by specific epitopes present on BSA's sequence. Furthermore, comparing scaffolds with different BSA/HSA ratios for their mechanical properties, wettability and ability to support cell adhesion and proliferation, we intended, using the  $\text{Ca}^{2+}$ -induced cold gelation technique, to set the basis for multivalent tunable scaffolds adaptable to several types of cells and tissues.

## 2. Materials and methods

### 2.1. Materials

BSA, HSA, Casein Sodium Salt from bovine milk were obtained from Sigma-Aldrich, Spain and used without further purification. All other reagents were analytical grade and purchased from Sigma-Aldrich, Spain.

### 2.2. Scaffolds preparation

The scaffolds were obtained by salt-induced cold gelation in the presence of calcium chloride ( $\text{CaCl}_2$ ) and DL-Dithiothreitol (DTT) at pH 7.07 as described previously [4]. Shortly, protein solutions of BSA and HSA in water and Casein in Tris50 mM pH 7.4 were used for the scaffolds. The solutions were heated at 60 °C for 30 min. After cooling, the protein solutions at room temperature for 1 h,  $\text{CaCl}_2$  (25 mM) and DTT (25 mM) were added and the mixtures were stirred to homogenize the samples. The resulting solutions were cast on 24-well plates, left gel overnight and frozen at –20 °C for 2 days and freeze dried for 3 days to remove the solvent completely. Resulting scaffolds with a diameter of 14 mm and a height of 9 mm were macroscopically opaque white and robust enough to be easily handle without breaking during experiments (Fig. 1). Scaffolds were kept at room temperature until further use.

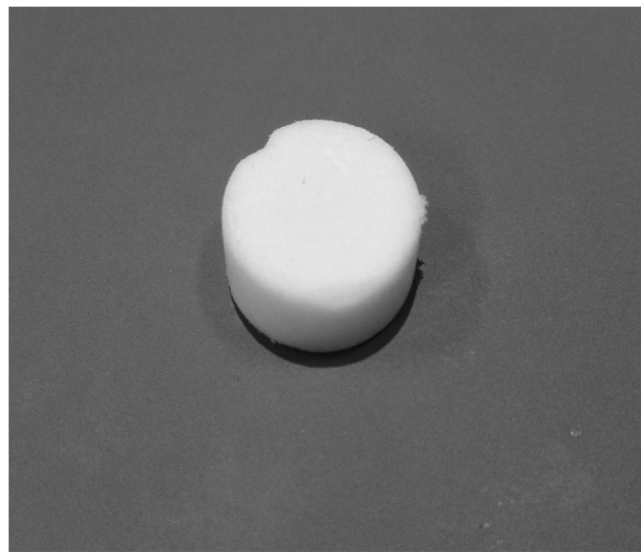


**Fig. 1.** Macroscopic image of the BSA25%HSA75% scaffold.

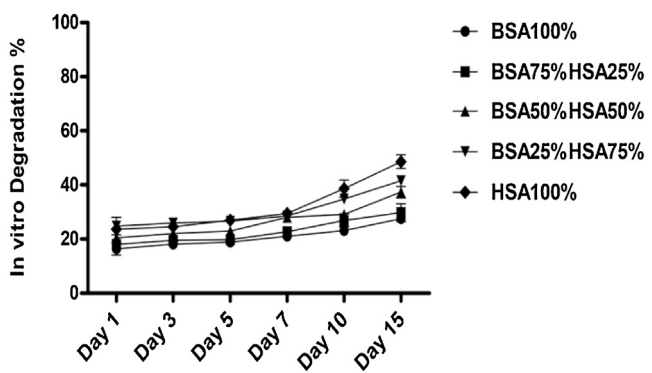


**Fig. 2.** *In vitro* degradation of the scaffolds incubated in PBS at pH 7.4 for 1, 3, 5, 7, 10 and 15 days at 37 °C. Data were reported as mean  $\pm$  SD of three independent experiments, each with triplicates.

Total protein content (4.19% w/v of BSA and 0.69% w/v of casein) of scaffolds was previously determined regarding optimal responses for *in vitro* degradation, swelling ratio, porosity, pore size and cell viability [4]. The new set of scaffolds were obtained by incremental substitution of BSA by HSA while maintaining constant the amount of casein. For a better comprehension of the degree of substitution the maximum amount of BSA (4.19%) was defined as 100% and casein was omitted from the formulation. The incremental replacement of BSA by HSA resulted in five BS<sub>Ax</sub>/HS<sub>Ay</sub> scaffolds: BSA100%, BSA75%HSA25%, BSA50%HSA50%, BSA25%HSA75% and HSA100%.

### 2.3. Contact angle

Contact angle measurements (sessile drop in dynamic mode) were performed at room temperature in a Data Physics OCA20 device using ultrapure water as test liquid. The contact angles were measured by depositing ultrapure water drops (3  $\mu\text{l}$ ) on the sample surface and analyzed with SCA20 software. At least five measurements in each sample were performed in different scaffold surface locations and the average contact angle was taken as the result for each sample.

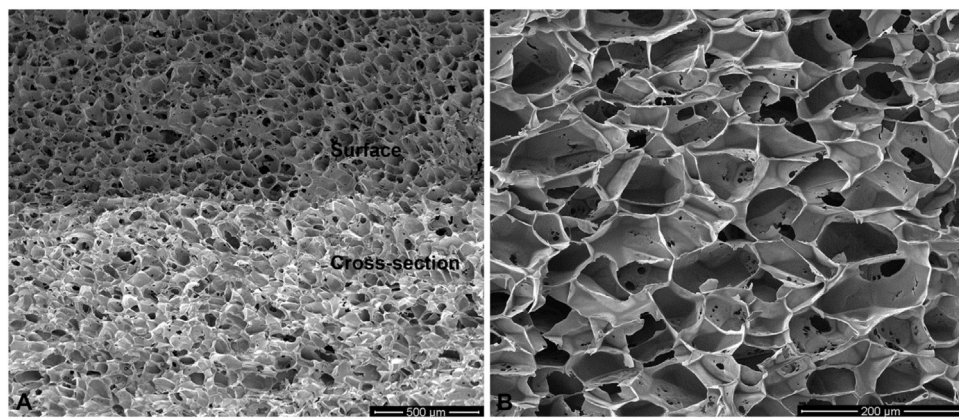


**Fig. 3.** SEM micrographs of BSA25% HSA75% scaffolds: General view (A) and cross-sectional view (B).

#### 2.4. Swelling degree

The degree of swelling was assessed by measuring the difference in weight between dry and swollen samples. The dry scaffolds were immersed in PBS at pH 7.4 at 37 °C for 24 h. After removal of excess of buffer, the wet weight of the scaffolds was determined. The swelling degree was calculated as follows and expressed in terms of percentage to the dry sample:

$$\text{swellingdegree} (\%) = \left( \frac{W_s - W_d}{W_d} \right) \times 100$$

where  $W_s$  is the mass of the swollen material, and  $W_d$  is the initial dry mass.

#### 2.5. In vitro degradation

The set of scaffolds were incubated at 37 °C in PBS at pH 7.4, for 15 days. Solutions were changed every 24 h and at designated time points, samples were washed thoroughly with distilled water, dried in a desiccator, and weighed to estimate the extent of degradation by the following equation:

$$\text{weightloss} (\%) = \left( \frac{m_i - m_f}{m_i} \right) \times 100$$

where  $m_i$  is the initial dry mass of the sample and  $m_f$  is the final dry mass.

#### 2.6. Scaffolds porosity

The porosity of the scaffolds was determined in the swollen state in water using the following equation

$$\text{porosity} (\%) = \left( \frac{W_s - W_d}{d_{\text{water}}} \right) \times \frac{100}{V}$$

where  $W_s$  and  $W_d$  are the mass of the swollen and lyophilized scaffold, respectively,  $d_{\text{water}}$  is the density of pure water, and  $V = (\pi r^2 h)$  is the measured volume of the scaffold in the swollen state. All measurements were taken 24 h after soaking the scaffolds in water at 37 °C using a paquimeter. Excess surface water was removed with a filter paper before each measurement.

#### 2.7. Microstructural morphology

Freeze-dried BS<sub>Ax</sub>/HS<sub>Ay</sub> scaffolds were fractured after immersion in liquid nitrogen. All samples were coated with 80%Au and 20% Pd and observed at 5.0 kV with SEM (NOVA NanSEM 200 FEI). The mean pore size and wall thickness was estimated using Image J software with at least 10 pores in three different spots.

#### 2.8. Secondary structure analysis

Infrared (FTIR) spectra were acquired at room temperature with a FTIR Spectrum BX (Perkin Elmer) with attenuated total reflection mode (ATR) Miracle (Pike). FTIR spectra were collected after 16 scans with a resolution of 4 cm<sup>-1</sup> from 4000 to 600 cm<sup>-1</sup>.

FTIR-derived convoluted curves, corresponding to Amide I spectral interval of [1600; 1720] cm<sup>-1</sup>, were processed in "Feat Peaks (Pro)" routine of "Peak Analyzer" menu in OriginPro software, v.8.5.0 (OriginLab Corporation, USA). For each convoluted curve, no smoothing was performed prior to fitting. The baseline subtraction was followed by a multiple pass fit. Discrete initial peak spectral positions, used for fitting, were identified by a Second Derivative built-in method. The secondary conformational data, resulting from individual peaks, were obtained based on the reported peak assignments [13].

#### 2.9. Dynamic Mechanical Analysis (DMA)

The viscoelastic measurements of the scaffolds were performed using a TRITEC8000B DMA (Triton Technology, UK), equipped with the compressive mode. All samples were immersed in PBS overnight before measurement. DMA spectra were obtained during a frequency scan ranging between 0.1 and 10 Hz for all time points. The experiments were performed under constant strain amplitude, corresponding to approximately 1% of the original height of the sample. Samples were tested under close physiological conditions, i.e. immersed in PBS and at 37 °C.

#### 2.10. Cell culture

The BJ-5ta cell line (normal human skin fibroblasts immortalized by overexpression of telomerase) was maintained according to ATCC recommendations (four parts of Dulbecco's modified Eagle's medium (DMEM) containing 4 mmol/l-glutamine, 4.5 g/L sodium bicarbonate and 1 part of Medium 199, supplemented with 10% (v/v) of fetal bovine serum (FBS), 1% (v/v) of penicillin/streptomycin solution and 10 µg/ml hygromycin B). Cells were maintained at 37 °C in a humidified atmosphere with 5% CO<sub>2</sub> and culture medium was replaced every 2 days.

#### 2.11. Cytotoxicity evaluation

BJ-5ta cells were used as model of general cytotoxicity. Cytotoxicity induced by degradation products and leachables from the scaffolds was evaluated by exposing cells to culture medium conditioned by 24 h contact with the scaffolds.

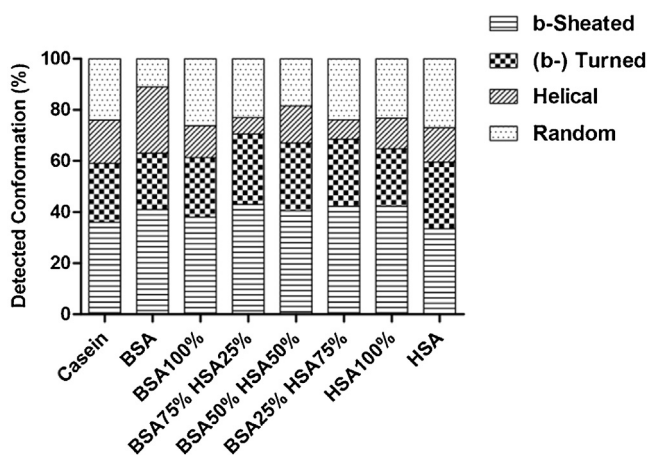


**Fig. 4.** Secondary structural conformations of the scaffolds elucidated by “deconvolution” of Amide I spectral region. Casein, BSA and HSA correspond to the controls. The variations of BSA and HSA content of the scaffolds are denoted by numbers, following the abbreviations.

Scaffolds were disinfected by immersion (3X) in PBS supplemented with 1% (v/v) PS for 20 min. The conditioned media were obtained by incubating the disinfected scaffolds in 2 ml of medium at 37 °C in a humidified atmosphere of 5% CO<sub>2</sub> for 24 h.

Cells were seeded at a density of 10 × 10<sup>3</sup> cells/100 µl/well on 96-well tissue culture polystyrene (TCPS) plates (TPP, Trasadingen, Switzerland) the day before experiments and then exposed to the conditioned medium and further incubated. At the end of 24 and 48 h of contact, metabolic viability was assessed using the MTT (3-(4,5-dimethylthiazol-2-yl)-2,5-diphenyltetrazoliumbromide) assay [14].

## 2.12. Cell culture in the scaffolds

The influence of scaffold composition on skin fibroblasts cell proliferation was assessed by quantifying DNA content.

The BSAX/HSAy disinfected scaffolds were equilibrated for 24 h in medium without FBS at 37 °C in a humidified atmosphere of 5% CO<sub>2</sub>. The scaffolds were gently placed in 24-well (TCPS) plates (TPP, Trasadingen, Switzerland) then 200 µl of cell suspension (5 × 10<sup>5</sup> cells/ml) were loaded onto the upper side of each scaffold and allowed to infiltrate into the scaffold. After 1 h incubation, 1 ml of fresh medium was added to each scaffold and the plate was incubated at 37 °C with 5% CO<sub>2</sub> for either 120 or 192 h. Half of culture media was renewed every 2 days.

At the end of each time point, cells/scaffold constructs were collected, rinsed twice with warm PBS. Cells were collected by incubation of the cells/scaffold constructs with trypsin. To ensure the collection of all cells from the scaffold the constructs were incubated 3 times in trypsin. Cell proliferation was assessed in terms of DNA content quantified with Hoechsts 33258 (Invitrogen, CA) as previously described [4].

## 2.13. Statistical analysis

Data are presented as average standard deviation (SD), n = 3. Statistical comparisons were performed by one-way ANOVA with GraphPad Prism 5.0 software (La Jolla, CA, U.S.A.). Tukey's posthoc test was used to compare all the results between them, and a Dunnett's test was used to compare the results with a specific control. A P-value of < 0.05 was considered to be statistically significant.

**Table 1**

Contact angle of the scaffolds performed at room temperature with ultrapure water as test liquid.

Scaffold	0°	15°	30°	45°	1'
BSA100%	98.4 ± 1.1	92.4 ± 2.3	90.8 ± 2.1	85.9 ± 1.3	85.7 ± 4.1
BSA75%HSA25%	98.9 ± 2.5	93.7 ± 1.1	93.3 ± 4.5	87.1 ± 1.1	84.9 ± 3.7
BSA50%HSA50%	95.3 ± 1.3	84.6 ± 1.3	75.9 ± 3.8	40.6 ± 3.3	—
BSA25%HSA75%	83.7 ± 3.4	79.4 ± 2.3	65.0 ± 6.2	20.9 ± 1.6	—
HSA100%	80.6 ± 0.7	60.7 ± 4.5	—	—	—

## 3. Results and discussion

The ideal choice of both cell and scaffold sources varies in relation to the specific tissue to be engineered, and these are intrinsic in effective tissue engineering. The production of an engineered tissue *in vitro* requires the use of cells to populate matrices and produce matrices resembling that of the native tissue [15]. The cells can be isolated from the tissue of the patient however more recently stem cells that will differentiate into the target tissue are widely used.

Regardless of the source of the cells, the physical properties of the scaffolds are crucial for the success of a tissue engineering strategy, as they should match or mimic the physical properties of the target tissue.

Usually tissue engineering research focuses on the design and development of scaffolds for a specific type of cells. The novelty of the work presented here focuses on the design of a tunable scaffold formulation that can support the adhesion and proliferation of different types of cells.

Setting the BSA4.19%/Casein0.69% scaffold formulation defined as BSA100%, which previously demonstrated to be suitable for tissue engineering applications [4], as the starting formulation, a set of five scaffolds (BSA100%, BSA75%HSA25%, BSA50%HSA50%, BSA25%HSA75% and HSA100%) were obtained by the incremental replacement of BSA by HSA.

The BSAX/HSAy scaffolds (Fig. 1) were fully characterized regarding their physical properties and ability to support cell growth. Furthermore, their mechanical performances in terms of storage modulus and loss factor were compared with the mechanical performances of several types of tissues described in the literature to check the tunability of the scaffold formulation and its potential to be used for different tissue types.

### 3.1. Contact angle

As surface hydrophobicity is related to differential cell adhesion, indirectly through protein binding, it is of particular interest to study and understand the materials' surface behavior in contact with hydrated media. An adequate level of surface wettability is desirable for optimal cell attachment or releasing since the differential adsorption of cell interactive glycoproteins from serum containing media, depend on surface hydrophobicity [16].

The surface wettability of the BSAX/HSAy scaffolds was assessed by measuring the contact angle through spread of a water droplet. In Table 1 are presented the water contact angle values obtained for each scaffold.

Considering the porous surface of the scaffolds which creates a capillary effect influencing the precision of contact angle measurements, only time zero was considered for better comparison between scaffolds.

Cell adhesion into scaffolds depends on several parameters which vary depending on the type of cells to be seeded. Despite there is not an ideal contact angle that promotes cell adhesion there are several studies which demonstrate that optimal contact angle values should be within 60° and 80° [17,18].

At time zero, the BSA25%HSA75% and HSA100% scaffolds presented contact angles of almost 80°, close to the optimal conditions

**Table 2**

Degree of swelling and *in vitro* degradation of the scaffolds incubated in PBS at pH 7.4 for 24 h and 15 days, respectively, at 37 °C.<sup>a</sup>

Scaffold	Swelling degree (%)	<i>In vitro</i> degradation (%)
BSA100%	876 ± 64	27.53 ± 1.87
BSA75%HSA25%	951 ± 156	29.77 ± 3.31
BSA50%HSA50%	1197 ± 102	37.34 ± 2.11
BSA25%HSA75%	1204 ± 150	41.54 ± 1.05
HSA100%	1221 ± 89	48.56 ± 2.55

<sup>a</sup> Data reported as mean ± SD of three independent experiments, each with triplicates.

for cell adhesion and growth, while for the others BSAX/HSAy scaffolds the calculated water contact angle was above the optimal range. Nevertheless, within the first minute of contact, all the scaffolds had wet surfaces favorable for cell adhesion.

It is also possible to observe a general trend toward a decrease on scaffold hydrophobicity increasing the replacement of BSA by HSA. The scaffolds with 100% BSA and 100% HSA were respectively the more hydrophobic and more hydrophilic.

This difference in hydrophobicity of structures with BSA and HSA was described before by Egbaria and Friedman in 1992 when using different dyes. They suggested that BSA microspheres were more hydrophobic than HSA and ovalbumin microspheres [19].

Despite the high homology between the two albumins there are some differences; BSA has 582 amino acid residues while HSA has 585 and the net charge is –17 for the first and –15 for the second [20].

Regardless of these differences the decrease on hydrophobicity when the BSA was replaced by HSA was most likely related with differences in amino acidic composition between the two albumins. HSA has only one tryptophan equivalent to a BSA tryptophan, buried in a hydrophobic pocket, while BSA has one additional tryptophan which is more exposed to solvents [20].

There is also a significant difference in the primary sequences of the two albumins corresponding to the C-terminals and their three-dimensional arrangements. The C-terminal helical rod of HSA is amphiphilic with the hydrophilic residues on a half-side of the rod and the hydrophobic ones on the other side. In contrast, the C-terminal rod of BSA is rather hydrophobic as whole. This difference comes from the fact that HSA has one more lysine and glutamic acid residues than BSA [21].

These differences, on the amino acidic content and distribution in the primary sequence, could support the trend on the hydrophobic behavior of the BSAX/HSAy scaffolds.

### 3.2. Swelling degree and *in vitro* degradation

The ability of a scaffold to swell in the presence of water influences the absorption of body fluids and transfer of nutrients and metabolites in the cells milieu. The swelling, which strongly depends on the hydrophobic nature of the constituent materials and microstructure of the scaffold, affects, apart from cell adhesion and proliferation, scaffold's degradation rates and mechanical strength [22].

Therefore, the BSAX/HSAy scaffolds were characterized for degree of swelling and *in vitro* degradation by immersion of the scaffolds in PBS pH 7.4 at 37 °C. The results regarding the swelling degree after 24 h of incubation and *in vitro* degradation determined at the end of 15 days are presented on Table 2.

As expected, considering the strong influence of hydrophobicity on the analyzed parameters, there was an increase on the swelling degree and *in vitro* degradation with the incremental substitution of BSA by HSA. The HSA100% scaffold had the highest swelling degree (1221 ± 89%) and *in vitro* degradation (48.56 ± 2.55%) which

**Table 3**

Pore medium size and wall thickness determined by SEM micrographs observations of scaffolds surface and cross-sectional views.<sup>a</sup>

	Surface (μm)	Cross-section (μm)	Wall (μm)
BSA100%	117 ± 26	109 ± 18	4.94 ± 1.59
BSA75%HSA25%	121 ± 15	114 ± 20	4.91 ± 1.40
BSA50%HSA50%	114 ± 9	110 ± 14	4.90 ± 1.50
BSA25%HSA75%	105 ± 11	101 ± 10	3.24 ± 0.78
HSA100%	102 ± 11	103 ± 10	3.04 ± 0.49

<sup>a</sup> Data reported as mean ± SD (n = 15).

was explained by the lowest hydrophobicity of this scaffold when compared with the other BSAX/HSAy scaffolds.

A more hydrophilic material is more capable of uptaking water which results in higher swelling degrees thus influencing the degradation rates of systems constituted by the material. As HSA is more hydrophilic than BSA, the scaffolds with higher HSA contents will be able to swell more and will present higher degradation rates as consequence of the greater affinity of HSA towards water.

Scaffolds' degradation profiles should allow cells to adapt to the body environment and ideally match the rate at which the extracellular matrix replaces the scaffold while maintaining its mechanical properties and porosity.

Despite the distinct final degradation ratios there were no differences across the degradation profiles of the BSAX/HSAy scaffolds (Fig. 2).

After one day of incubation the degradation rates were around 20% with some variation according to the different scaffold hydrophobicity. The degradation rates were maintained between 20 and 30% until day 7 with a slight increase for all the scaffolds. From this day up to the final time point, the degradation profiles were more pronounced mainly for the scaffolds with higher HSA content.

Previously we have shown the influence of BSA and casein amount as well the pH at which the scaffolds were prepared in the swelling properties and *in vitro* degradation rates [4]. As the total amount of protein was maintained constant throughout the set of the BSAX/HSAy scaffolds, the differences in swelling degrees and *in vitro* degradation rates can be attributed to the replacement of BSA by HSA, which confirms the role of the scaffolds' hydrophobicity on the respective swelling degrees and degradation rates.

### 3.3. Microstructural morphology and porosity

Pore structure must be considered when developing scaffolds for tissue engineering as they should have a porous architecture with high surface area for maximum cell loading and cell-matrix interactions, as well as nutrient and oxygen flow [23].

If pores are too small, apart from a limited diffusion of nutrients and waste, cell migration is limited, which results in the formation of a cellular capsule surrounding the scaffold. On the other hand, if pores are too large, the surface area is reduced which limits cell adhesion [24]. Pore morphology also affects the scaffold degradation kinetics and the mechanical properties.

The porosity of BSAX/HSAy scaffolds was quantified in the swollen state after soaking the samples in water at 37 °C for 24 h. The protein based scaffolds showed porosity values between 81.8 ± 2.3% and 85.3 ± 3.4%. Despite the differences were not significant, there was a slight increase in the porosity of the scaffolds with increasing the degree of substitution.

The pore sizes and respective wall thickness of BSAX/HSAy scaffolds were measured analyzing SEM micrographs both at the surface and in cross-sectional views. The results presented on Table 3 showed a tendency, although not significant, towards reduced pore sizes and thinner walls with increasing HSA concentration. Such relation was most likely due to the higher

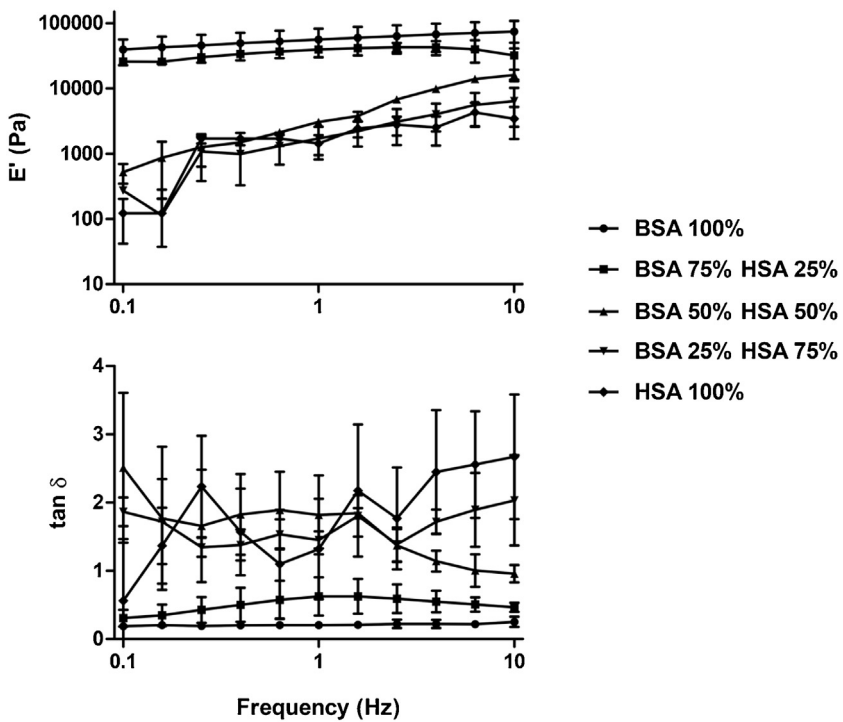


**Fig. 5.** Storage modulus ( $E'$ ) and loss factor ( $\tan \delta$ ) values for the scaffolds, obtained under immersion in PBS at 37 °C.

hydrophilicity of the human albumin. For the same volume, a material which is more hydrophilic will become more distributed when in contact with water than a hydrophobic material. The thinner walls of BSA25%HSA75% and HSA100% scaffolds resulted in a wider distribution of the proteins leading to the formation of smaller pores with consequent increased surface area of contact with water.

Independently of the degree of substitution of BSA by HSA, the pore size, shape and distribution were homogeneous both at the surface and in the cross-section. The porous structure of the BSA25%HSA75% scaffold observable in the SEM micrographs in Fig. 3 shows its high porosity and the uniformity of the microstructure. The other BS<sub>x</sub>/HS<sub>y</sub> scaffolds also presented a highly porous and uniform microstructural morphology (data not shown).

#### 3.4. Scaffolds' proteins secondary structure

Amide I spectral shape is known to possess good sensitivity to the amount and type of secondary structures, and is not strongly influenced by side chains [25]. Amide I vibrational spectra are therefore commonly used in secondary structure determinations. Inconsistencies in FTIR measurement and the treatment of acquired data, found in different papers dealing with lyophilized BSA [26], HAS [27] and casein [28], forced us to use the protocol, described in methods. Although the ultimate band assignment was performed according to Kong [13], the results presented in the three aforementioned reports were also considered. The resulting discrete peaks, their respective contribution to the overall FTIR-derived curves and the corresponding structural assignments are presented on Table 4.

Four types of resulting protein conformations are presented in Fig. 4. Random is defined as unordered conformation; Helical can be either  $\alpha$ - or 310-helix;  $\beta$ -turned is generally associated with  $\beta$ -sheets, as they can serve as  $\beta$ -sheet folding centers. The dense hydrophobic structure of  $\beta$ -sheet is designated as “ $\beta$ -Sheeted”.

Fig. 4 reveals a tendency towards less stable structure when comparing the BSA control (unblended) with the HSA control (unblended). It is worth noticing that the helical structure, defined for all the scaffolds, except BSA-control, is 310-helix. For BSA-

control the  $\alpha$ -helix is considered more stable than the 310 intermediate conformation [29].

Despite the tendency between the controls, a less pronounced tendency towards destabilization is observed in the BSA/HSA/CAS blended group.

BSA100% is unusually low in terms of  $\beta$ -related, hydrophobic content. However, starting from BSA75% towards a subtle but constant decrease in hydrophobic content is seen. Indeed, it was clearly demonstrated by swelling degree analysis and *in vitro* degradation that lower BSA content leads to a less stable scaffold. Yet, during the lyophilization, cold unfolding [30] and related protein reorganizations [31] occur, resulting in apparent structural uniformity, as reported by FTIR-derived analysis. Moreover, several unique features of the produced scaffolds, like porosity and thickness cannot be evaluated by the secondary structural analysis, yet they significantly influence other tested parameters.

#### 3.5. DMA

Cells that constitute most biological tissues require attachment to solid substrates to be viable (adherent cells). These solid substrates are usually viscoelastic, *i.e.*, their behavior has an elastic component, and they also show the ability to absorb mechanical energy (viscous component). In the human body, the range of elastic modulus and damping properties found in different tissues is wide. The classification of solid tissue includes stiff tissues (bone and teeth), hard connective tissues (cartilage and intervertebral discs), as well as soft tissues (skin, brain and adipose tissue). The damping properties of some human tissues were studied and it was concluded that practically all tissues are viscoelastic [32] and their damping properties vary according to the organ function.

We applied factorial design in order to study the effect of substituting BSA by HSA in the set of scaffolds. DMA is an adequate tool to characterize the viscoelastic properties of polymeric materials. Experiments were performed in a hydrated environment and body temperature, in an array of biologically relevant frequencies, in order to assess how samples behave in physiological-like envi-

**Table 4**

Resulting discrete peaks, their respective contribution to the overall FTIR-derived curves and the corresponding structural assignments.

Scaffold	Deconvoluted data		Deconvoluted data assignment			
	Peak center, cm <sup>-1</sup>	Area occupied, %	β-Sheeted	(β-)Turned	Helical	Random
Casein	1614	11	+			
	1621	8	+			
	1627	9	+			
	1634	8	+			
	1644	20.5				+
	1651	3.5				+
	1659	17			+	
	1667	2.5		+		
	1673	8.5		+		
	1681	2		+		
	1687	10		+		
BSA	1617	13	+			
	1623	4	+			
	1635	24	+			
	1645	10				+
	1651	1				+
	1657	26				+ <sup>a</sup>
	1667	0.5		+		
	1672	9		+		
	1681	0.5		+		
	1686	12		+		
BSA 100%	1614	11	+			
	1620	6	+			
	1625	0.5	+			
	1632	20.5	+			
	1644	18				+
	1652	8.25				+
	1660	12.5			+	
	1668	4.25		+		
	1674	4.5		+		
	1682	14.5		+		
BSA 75% HSA 25%	1614	12.5	+			
	1622	8	+			
	1634	22.5	+			
	1644	10				+
	1652	13				+
	1660	6.5				+
	1667	13.5		+		
	1676	1		+		
	1682	13		+		
BSA 50% HSA 50%	1608	6	+			
	1613	1	+			
	1622	17	+			
	1634	16.5	+			
	1644	12.5				+
	1651	6				+
	1658	14.5				+ <sup>a</sup>
	1667	15		+		
	1676	4		+		
	1688	7.5		+		
BSA 25% HSA 75%	1614	12.25	+			
	1622	10	+			
	1634	20	+			
	1644	11.3				+
	1652	12.5				+
	1660	7.6				+ <sup>a</sup>
	1668	12.3		+		
	1682	14		+		
HSA 100%	1614	12	+			
	1622	11.3	+			
	1634	19	+			
	1644	6.7				+
	1652	16.5				+
	1658	12				+ <sup>a</sup>
	1668	8.5		+		
	1682	14		+		

Table 4 (Continued)

Scaffold	Deconvoluted data		Deconvoluted data assignment			
	Peak center, cm <sup>-1</sup>	Area occupied, %	β-Sheeted	(β-)Turned	Helical	Random
HSA	1612	6	+			
	1623	12.5	+			
	1626	3	+			
	1634	12	+			
	1644	19				+
	1651	8				+
	1658	13.5			+	
	1666	6.5		+		
	1674	7.5		+		
	1684	12		+		

<sup>a</sup> The only α-helix was encountered for BSA control sample.

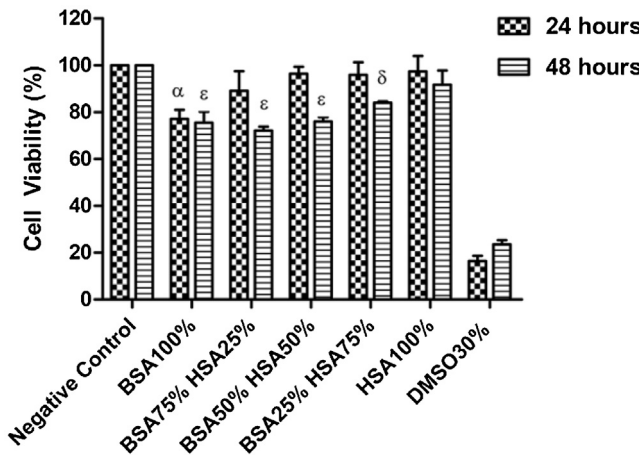


**Fig. 6.** BJ-5ta cell viability measured by MTT assay at 24 and 48 h of culture with undiluted conditioned medium pre-conditioned by contact with scaffolds for 24 h. The data represents mean  $\pm$  SD of three independent experiments, each with triplicates.  $\alpha P \leq 0.001$  when compared with negative control 24 h,  $\delta P \leq 0.001$  when compared with negative control 48 h,  $\varepsilon P \leq 0.001$  when compared with negative control 48 h.

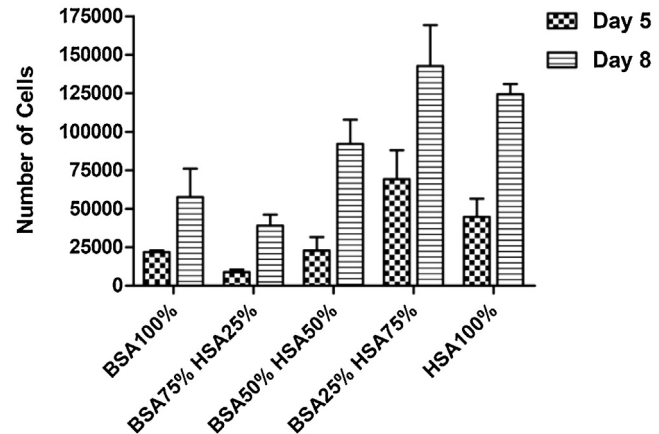


**Fig. 7.** Cell adhesion and growth on the scaffolds 5 and 8 days after seeding. The number of cells in each sample was indirectly measured by interpolation of their relative fluorescence, given by DNA intercalating probe Hoechst 33258 against a DNA standard curve. The data represents mean  $\pm$  SD of two independent experiments, each with triplicates.

ronment. Both storage (elastic) modulus,  $E'$ , and the loss factor,  $\tan \delta$  were obtained at different frequencies and are presented in Fig. 5.  $E'$  is a measure of the materials' stiffness while loss factor is the ratio of the amount of energy dissipated (viscous component) relative to stored energy (elastic component),  $\tan \delta = E'/E''$ .

The BSA100% scaffolds showed the highest  $E'$  values (e.g.,  $56 \pm 26$  kPa at 1 Hz) which were kept almost constant along the frequency range. Elastic modulus in this range can be found in the osteoid (i.e. pre-mineralized bone) [33] and in cartilage [34]. These

scaffolds showed a loss factor value of  $0.20 \pm 0.04$ , within the range of  $\tan \delta$  typical of bone [35,36]. The substitution of 25% BSA by HSA in the total mass of the scaffold (BSA75%HSA25% scaffold) led to a statistically significant decrease in the value of  $E'$  (e.g.,  $40 \pm 2.9$  kPa at 1 Hz). These values are in the range of what was previously measured in muscle [37]. The  $E'$  values were kept approximately constant along the frequency range. An increase in the loss factor value for the BSA75%HSA25% condition to  $0.6 \pm 0.27$ , at 1 Hz, was observed, showing an increase in the viscous component of these scaffolds.

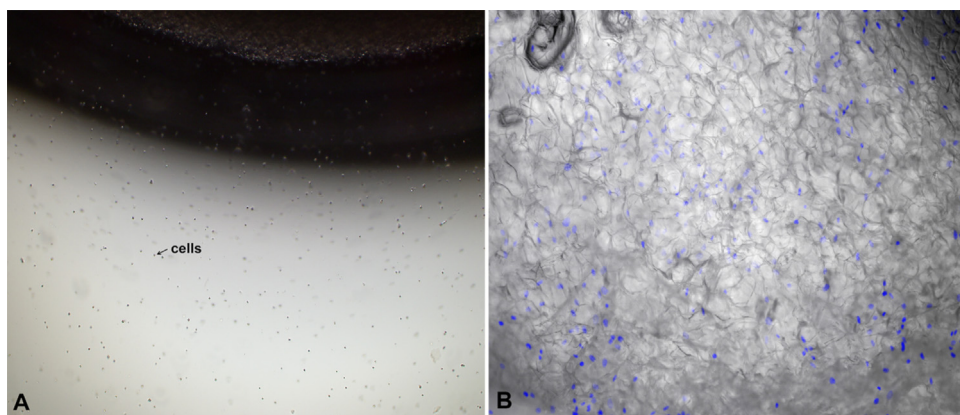


**Fig. 8.** Optical (A) and Fluorescence microscopy analyses of BJ-5ta cells seeded in the BSA25%HSA75% scaffold after 8 days of incubations: Cells being removed from the scaffold after trypsinization (A) and nuclei of cells growing in the scaffolds stained with Hoechst 33258 (B).

A drastic reduction in the values of  $E'$  was observed upon the substitution of 50% of BSA.  $E'$  values decreased one order of magnitude, to  $3.0 \pm 0.1$  kPa at 1 Hz. The successive additions of HSA, corresponding to 75% and 100% of substitution on the albumin mass, led to a decrease of  $E'$ , to  $1.7 \pm 0.8$  kPa and  $1.4 \pm 0.4$  kPa, respectively. These values are similar to the measured for neural tissue [33,38] and human skin, epidermis from both the thighs and forearm [39], and dermis [40].

### 3.6. Cell viability and proliferation

Ideally a scaffold should facilitate cell attachment and proliferation. Nonetheless the biocompatibility of the materials which composes the scaffold is critical. Neither the substrate materials nor its degradation by-products should elicit an inflammatory response nor demonstrate cytotoxicity [1].

To evaluate the cytotoxicity induced by constituents and leachables from the BSAX/HSAy scaffolds, BJ-5ta fibroblasts were exposed to undiluted culture medium pre-conditioned by contact with the scaffolds for 24 h.

The results of the indirect contact study after fibroblasts incubation for 24 and 48 h with materials' leachables, depicted in Fig. 6, showed some variations and trends in cell viability along time and with the degree of replacement of BSA by HSA.

There was a general decrease in cellular metabolic activity with exposure time, with statistical significance for BSAT75%HSA25% ( $P \leq 0.01$ ) and BSA50%HSA50% ( $P \leq 0.001$ ) scaffolds when comparing 24 h with 48 h of incubation. Besides scaffold composition, as long term effect, the reduction in viability could be related with the degradation of nutrients from the culture medium since it was maintained at 37 °C during pre-conditioning.

Furthermore, more extensive replacement had a positive effect on cell viability. Fibroblasts in contact with the HSA100% scaffold leachables had similar viability as compared to fibroblasts in contact with unconditioned medium (negative control). The trend towards higher cell viability with increasing HSA content supports the purpose of replacing the BSA by HSA on the original scaffold formulation.

Despite the variations in cell viability with time of incubation and degree of replacement, the values obtained with the indirect contact showed that the products and leachables released from the BSAX/HSAy scaffolds were not significantly toxic to cells.

To evaluate how BSAX/HSAy scaffolds support cell adhesion and proliferation, BJ-5ta foreskin fibroblasts were seeded on the scaffolds and grown for 5 and 8 days. Cell proliferation was determined in terms of DNA content measured with Hoechst 33258, a DNA intercalating fluorescent probe. The number of cells in each scaffold was indirectly measured by interpolation of the relative fluorescence value against a DNA standard curve ( $Y = 0.0002X + 23.129$ ;  $R^2 = 0.986$ ) constructed using known numbers of cells.

Fig. 7 shows the proliferation profile of BJ-5ta fibroblasts seeded on the BSAX/HSAy scaffolds, after 5 and 8 days of cell culture.

Fig. 7 demonstrates that the degree of substitution of BSA by HSA had a positive effect on BJ-5ta cell attachment and proliferation, after 5 and 8 days of incubation. This effect was more evident when comparing the BSA100% and BSA75%HSA25% scaffolds with the scaffolds with the highest degrees of substitution. Nevertheless, in both time points all the scaffolds were suitable for cell culture.

For the BSA25%HSA75% and HSA100% scaffolds despite noticeable difference in cell number between the two, was not statistically significant.

The improvement in foreskin fibroblasts growth within the scaffolds may be attributed to the increased hydrophilicity of the scaffolds with more extensive replacement of BSA, to the surface area provided by the scaffolds as well as to the viscoelastic properties of the scaffolds.

The BSA25%HSA75% and the HSA100% scaffolds presented contact angles around 80°, within the described optimal contact angles for cell adhesion [17,18]. These scaffolds also presented the smallest pores thus providing higher surface areas. Hence the BSA25%HSA75% and HSA100% scaffolds probably stimulated the initial cell adhesion, resulting in a higher number of fibroblasts able to proliferate when compared to the other scaffolds.

Besides appropriate hydrophilicity and surface area, which influences the affinity of the scaffolds for cell attachment and proliferation, the BSA25%HSA75% and HSA100% scaffolds showed Elastic modulus similar to those measured for human skin, epidermis from both thighs and forearm [39], and dermis [40].

Considering the great influence of scaffold stiffness on cell behavior and ultimately in tissue quality, the results of adhesion and proliferation were consistent with the seeded cells. Regarding the viscoelastic properties these scaffolds were the most indicated for BJ-5ta foreskin fibroblasts.

At the end of 8 days of incubation, there was an increase in the number of cells growing in the BSAX/HSAy scaffolds, indicating that these scaffolds, regardless of the described differences, support cell adhesion and proliferation (Fig. 8).

## 4. Conclusions

This study has provided additional insight to what is described in the literature on the influence of composition on the physical properties of scaffolds as in cell adhesion and proliferation. The replacement of bovine by human albumin on the formulation results in scaffolds with higher surface wettability, higher degree of swelling, higher *in vitro* degradation and smaller pore size and wall thickness.

As the total concentration of protein in the scaffolds was maintained constant, the differences between the scaffolds were directly related with the degree of substitution of BSA by HSA.

Moreover, we showed that by varying the proportion of BSA/HSA, it was possible to obtain scaffolds with viscoelastic properties close to some native tissues, which was supported by the cell adhesion and proliferation results using foreskin fibroblasts.

Also, the results suggested that by exploring more BSA/HSA ratios it may be possible to tailor with more precision scaffolds with viscoelastic properties similar to distinct tissues. This would facilitate the integration of the scaffold in a particular tissue, as the cells are in contact with an environment similar to the original tissue. Furthermore, immediately after implantation the construct it would show a mechanical/viscoelastic response similar to the original organ.

In conclusion, using the  $\text{Ca}^{2+}$ -induced cold gelation and varying the scaffolds formulation taking into account the balance between the hydrophobicity and hydrophilicity of its constituents, is here described as a useful approach for the development of tunable scaffolds for tissue engineering and tissue restoration of several types of tissues and organs.

## Acknowledgements

This work was supported by FCT I.P through the strategic funding UID/BIO/04469/2013 and the strategic funding UID/BIA/04050/2013. Artur Ribeiro thanks FCT for the SFRHBP/98388/2013 grant.

## References

- [1] G. Chen, T. Ushida, T. Tateishi, Scaffold design for tissue engineering, *Macromol. Biosci.* 2 (2002) 67–77.

- [2] C.M. Bryant, D.J. McClements, Molecular basis of protein functionality with special consideration of cold-set gels derived from heat-denatured whey, *Trends Food Sci. Technol.* 9 (1998) 143–151.
- [3] S. Barbut, E.A. Foegeding, Ca<sup>2+</sup>-induced gelation of pre-heated whey protein isolate, *J. Food Sci.* 58 (1993) 867–871.
- [4] A.J.A.M. Ribeiro, A.C. Gomes, A. Cavaco-Paulo, Developing scaffolds for tissue engineering using the Ca<sup>2+</sup>-induced cold gelation by an experimental design approach, *J. Biomed. Mater. Res. Part B* 100B8 (2012) 2269–2278.
- [5] W.H. Dietmar, S. Michael, V.R. Makarand, Scaffold-based tissue engineering: rationale for computer-aided design and solid free-form fabrication systems, *Trends Biotechnol.* 22 (7) (2004) 354–362.
- [6] K. Hirayama, S. Hirayama, M. Furuya, K. Fukuhara, Rapid conformation and revision on the primary structure of bovine serum albumin by ESIMS and FRIT-FAB LC/MS, *Biochem. Biophys. Res. Commun.* 173 (1990) 639–646.
- [7] S. Mirapurkar, U.H. Nagvekar, N. Sivaprasad, Polyreactivity of monoclonal antibodies produced against thyroid stimulating hormone (hTSH), *J. Immunoassay Immunochem.* 28 (2007) 119–126.
- [8] O. Gutmann, R. Ruehlewein, S. Reinbold, R.F. Niekrawietz, Fast and reliable protein microarray production by a drop-in-drop technique, *Lab Chip* 5 (2005) 675–681.
- [9] M. Granstrom, M. Eriksson, G. Edevag, A sandwich ELISA for bovine serum in viral vaccines, *J. Biol. Stand.* 15 (1987) 193–197.
- [10] F. Galisteo-González, J.A. Molina-Bolívar, Systematic study on the preparation of BSA nanoparticles, *Colloids Surf. B* 123 (2014) 286–292.
- [11] S. Tanabe, Y. Kobayashi, F. Takahata, F. Morimatsu, R. Shibata, T. Nishimura, Some human B and T cell epitopes of bovine serum albumin, *Biochem. Biophys. Res. Commun.* 293 (2002) 1348–1353.
- [12] J. Serrano-Vicente, M.L. Caballero, R. Rodriguez-Perez, P. Carretero, R. Perez, J.G. Blanco, S. Juste, I. Moneo, Sensitization to serum albumins in children allergic to cow's milk and epithelia, *Pediatr. Allergy Immunol.* 18 (2007) 503–507.
- [13] J. Kong, S. Yu, Fourier transform infrared spectroscopic analysis of protein secondary structures, *Acta Biochim. Biophys. Sin.* 39 (8) (2007) 549–559.
- [14] Y. Liu, D. Schubert, Cytotoxic amyloid peptides inhibit cellular 3-(4,5-dimethylthiazol-2-yl)-2,5-diphenyltetrazolium bromide (MTT) reduction by enhancing MTT formazan exocytosis, *J. Neurochem.* 69 (1997) 2285–2293.
- [15] D. Howard, L.D. Buttery, K.M. Shakesheff, S.J. Roberts, Tissue engineering: strategies stem cells and scaffolds, *J. Anat.* 213 (1) (2008) 66–72.
- [16] B. Cortese, M.O. Riehle, S. D'Amone, G. Gigli, Influence of variable substrate geometry on wettability and cellular responses, *J. Colloid Interface Sci.* 394 (2013) 582–589.
- [17] S.H. Kim, H.J. Ha, Y.K. Ko, S.J. Yoon, Correlation of proliferation, morphology, and biological responses of fibroblasts on the LDPE with different surface wettability, *J. Biomater. Sci. Polym. Ed.* 18 (2007) 609–622.
- [18] L.C. Xu, Effect of surface wettability and contact time on protein adhesion to biomaterial surfaces, *Biomaterials* 28 (2007) 3273–3283.
- [19] K. Egbaria, M. Friedman, Physicochemical properties of albumin microspheres determined by spectroscopic studies, *J. Pharm. Sci.* 81 (2) (1992) 186–190.
- [20] D.C. Carter, J.X. Ho, Structure of serum-albumin, *Adv. Protein Chem.* 45 (1994) 153–203.
- [21] Y. Moriyama, K. Takeda, Reformation of the helical structure of human serum albumin by the addition of small amounts of sodium dodecyl sulfate after the disruption of the structure by urea. A comparison with bovine serum albumin, *Langmuir* 15 (1999) 2003–2008.
- [22] X. Feng, R. Pelton, Carboxymethyl cellulose: polyvinylamine complex hydrogel swelling, *Macromolecules* 40 (2007) 1624–1630.
- [23] X. Zhang, M.R. Reagan, D.L. Kaplan, Electrospun silk biomaterial scaffolds for regenerative medicine, *Adv. Drug Deliv. Rev.* 61 (2009) 988–1006.
- [24] C.M. Murphy, M.G. Haugh, F.J. O'Brien, The effect of mean pore size on cell attachment, proliferation and migration in collagen-glycosaminoglycan scaffolds for bone tissue engineering, *Biomaterials* 31 (2010) 461–466.
- [25] A. Barth, C. Zscherp, What vibrations tell us about proteins, *Q. Rev. Biophys.* 35 (4) (2002) 369–430.
- [26] K.G. Carrasquillo, R.A. Cordero, S. Ho, J.M. Franquiz, K. Griebelnow, Structure-guided encapsulation of bovine serum albumin in Poly(DL-lactic-co-glycolic) acid, *Pharm. Pharmacol. Commun.* 4 (12) (1998) 563–571.
- [27] R. Artali, A. Del Pra, E. Foresti, I.G. Lesci, N. Roveri, P. Sabatino, Adsorption of human serum albumin on the chrysotile surface: a molecular dynamics and spectroscopic investigation, *J. R. Soc. Interface* 5 (20) (2008) 273–283.
- [28] S.J. Prestrelski, N. Tedeschi, T. Arakawa, J.F. Carpenter, Dehydration-induced conformational transitions in proteins and their inhibition by stabilizers, *Biophys. J.* 65 (2) (1993) 661–671.
- [29] R.S. Vieira-Pires, J.H. Moraes-Cabral, 310 helices in channels and other membrane proteins, *J. Gen. Physiol.* 136 (6) (2010) 585–592.
- [30] F. Meersman, L. Smeller, K. Heremans, Comparative Fourier transform infrared spectroscopy study of cold-, pressure-, and heat-induced unfolding and aggregation of myoglobin, *Biophys. J.* 82 (5) (2002) 2635–2644.
- [31] S.V. Lale, M. Goyal, A.K. Bansal, Development of lyophilization cycle and effect of excipients on the stability of catalase during lyophilization, *Int. J. Pharm. Invest.* 1 (4) (2011) 214–221.
- [32] N. Sasaki, Viscoelastic properties of biological mater, in: Juan de Vicente (Ed.), Viscoelasticity—From Theory to Biological Applications, InTech, Rijeka, 2012, pp. 99–122.
- [33] A.J. Engler, S. Sen, H.L. Sweeney, D.E. Discher, Matrix elasticity directs stem cell lineage specification, *Cell* 126 (2006) 677–689.
- [34] G.R. Fulcher, D.W. Hukins, D.E. Shepherd, Viscoelastic properties of bovine articular cartilage attached to subchondral bone at high frequencies, *BMC Musculoskel. Disord.* 10 (2009) 61–68.
- [35] N. Sasaki, M. Yoshikawa, Stress relaxation in native and EDTA-treated bone as a function of mineral content, *J. Biomech.* 26 (1993) 77–83.
- [36] J.F. Mano, Viscoelastic properties of bone: mechanical spectroscopy studies on a chicken model, *Mater. Sci. Eng. C* 25 (2005) 145–152.
- [37] K. Chino, R. Akagi, M. Dohi, S. Fukashiro, H. Takahashi, Reliability and validity of quantifying absolute muscle hardness using ultrasound elastography, *PLoS One* 7 (2012) e45764–45768.
- [38] G.T. Fallenstein, V.D. Hulce, J.W. Melvin, Dynamic mechanical properties of human brain tissue, *J. Biomech.* 2 (1969) 217–226.
- [39] D.L. Bader, P. Bowker, Mechanical characteristics of skin and underlying tissues in vivo, *Biomaterials* 4 (1983) 305–308.
- [40] V.F. Achterberg, L. Buscemi, H. Diekmann, J. Smith-Clerc, H. Schwengler, J.J. Meister, H. Wenck, S. Gallinat, B. Hinz, The nano-scale mechanical properties of the extracellular matrix regulate dermal fibroblast function, *J. Invest. Dermatol.* 134 (2014) 1862–1872.